Arch Appl Mech (2010) 80: 581–592
DOI 10.1007/s00419-009-0327-9

ORIGINAL

Vladimir A. Osinov

Critical distances for the formation of strong discontinuities in fluid-saturated solids

Received: 19 March 2009 / Accepted: 24 April 2009 / Published online: 12 May 2009

Abstract An increase in the stiffness of a solid in compression is known to lead to the steepening of the profiles of compression waves and, as a consequence, to the formation of strong discontinuities from continuous waves propagating in the solid. In this paper, the critical distance required for a continuous wave to turn into a shock wave is calculated from the evolution equation for a weak discontinuity (acceleration wave) propagating into a quiescent region. Infinite growth of the amplitude of an acceleration wave in a finite time signifies the transition to a strong discontinuity. Relations between the critical distances for plane, cylindrical and spherical waves are established. Numerical examples are presented for a particular case of the pressure-dependent stiffness typical of granular solids such as sand or soil, with emphasis placed on the influence of a small amount of free gas in the pore fluid.

Keywords Critical distance · Strong discontinuity · Acceleration wave · Granular solid

1 Introduction

The stiffness of granular solids such as soils or powders depends on the current pressure and, being a tensorial quantity with rather complicated dependence on the stress state, has a general tendency to increase with increasing pressure. An increase in the stiffness in compression may also be observed in a fluid-saturated porous solid if, apart from the properties of the solid skeleton, the pore fluid is not a pure liquid but a liquid with a small amount of free gas whose compressibility is strongly pressure-dependent. The property of the stiffness to increase in compression makes the propagation of compression waves in dry or fluid-saturated granular solids similar to that in gases: a continuous compression wave propagating into a quiescent region steepens and turns into a shock wave after a finite time of propagation [1]. This so-called critical time determines the critical distance which a continuous compression front travels before it loses continuity. For a given medium, the critical time and the corresponding critical distance depend on the rate of the boundary loading and decrease with increasing rate. An estimation of the critical distance may be required in order to choose a proper computational strategy allowing for discontinuous solutions if the rate of loading is high enough to expect that the critical distance may lie within the range of distances considered in the problem under study.

For plane longitudinal waves propagating into a quiescent region in a medium with a nonlinear stress-strain relation, the solution has the structure of a so-called simple wave [1]. This makes it possible to trace the evolution of the gradient of the solution at each point of the wave front and thus to derive an explicit formula for the critical distance for a continuous front of arbitrary shape [2]. In many applications, the knowledge of the critical distance for plane waves alone does not suffice since the waves often have cylindrical or spherical symmetry rather than being plane. The aim of the present study is to calculate and compare the critical distances for plane, cylindrical and spherical longitudinal waves in a medium with pressure-dependent stiffness.

V. A. Osinov (✉)
Institute of Soil Mechanics and Rock Mechanics, University of Karlsruhe, 76128 Karlsruhe, Germany
E-mail: vladimir.osinov@ibf.uni-karlsruhe.de

In the case of cylindrical or spherical fronts the solution is not a simple wave. This fact does not allow us to derive a tractable equation for the gradients of the solution on the whole wave front as in [2]. To circumvent this difficulty, in the present paper we adopt a different approach: we consider the propagation of a weak discontinuity (a jump in the first derivatives of a continuous solution) rather than a smooth wave front.

The evolution of a weak discontinuity (an acceleration wave) depends on the constitutive behaviour of the medium and on the curvature of the surface of the discontinuity in space [3–5]. The amplitude of a weak discontinuity may become infinite after a finite time of propagation. Similar to smooth waves, this instant corresponds to the transition from the continuous solution to a shock wave and determines a critical distance. The coefficients in the evolution equation for the amplitude of an acceleration wave depend on the state of the medium in the domain into which the wave propagates. If the solution ahead of a front is known—in particular, if the discontinuity propagates into a quiescent region—the evolution equation for the amplitude can be solved directly. Although the acceleration-wave approach allows us to trace the evolution of the gradient of the solution only at the point of discontinuity, that is, at the leading point of the wave front rather than on the whole wave profile, an advantage of this method is that plane, cylindrical and spherical problems can be solved in a uniform way.

Besides deriving explicit formulae for the critical distances, in this paper we will give quantitative estimations of the critical distances assuming a particular form of the pressure dependence of the stiffness typical of granular solids such as sand or soil. Particular attention will be given to the presence of a small amount of free gas in the pore fluid, which strongly influences the compressibility of the solid and is therefore expected to influence the critical distance.

2 Evolution of weak discontinuities

Plane, cylindrical and spherical waves considered below are described by a system of quasilinear equations generally written in the form

$$\frac{\partial u_i}{\partial t} + A_{ij}(u_1,\dots,u_N)\frac{\partial u_j}{\partial x} = B_i(u_1,\dots,u_N,x), \quad i = 1,\dots,N, \tag{1}$$

where $u_1,\dots,u_N$ are unknown functions, and the variables x and t stand for a spatial coordinate and time, respectively. The coefficients of the system, A_{ij}, and the right-hand sides, B_i, are functions of u_i, and B_i may also depend explicitly on x. The functions $A_{ij}(u_1,\dots,u_N)$, $B_i(u_1,\dots,u_N,x)$ are assumed to have continuous first partial derivatives with respect to their arguments $u_1,\dots,u_N$ and x.

As is known, given continuous initial and boundary data, system (1) may have a continuous solution only within a finite time [6]. This holds for both smooth data and data with weak discontinuities. The evolution of the amplitude of a weak discontinuity for system (1) is shown to be described by an ordinary differential equation of the Bernoulli type [7–12]. The coefficients of this equation can be expressed in different ways. We will use the evolution equation in the form derived in [11,12]. The only difference between system (1) and the system considered in [11,12] is that the right-hand sides B_i in [11,12] do not depend explicitly on x. It can be shown that this dependence does not influence the evolution equation for the amplitude of a weak discontinuity if, as assumed above, the first partial derivatives of B_i with respect to the argument x are continuous.

If the first derivatives $\partial u_i/\partial x$, $\partial u_i/\partial t$ of a solution to (1) are discontinuous on a curve in the (x,t)-plane, this curve is necessarily a characteristic of system (1). The speed of propagation of the discontinuity front in space, c, is a (real) eigenvalue of the matrix A_{ij}. Let $[\![\ ]\!] = (\ )^+ - (\ )^-$ denote the jump in a quantity across the front, with $(\ )^+$ and $(\ )^-$ being the values ahead of and behind the front, respectively. The vector $[\![\partial u_i/\partial x]\!]$ is shown to be a right eigenvector of the matrix A_{ij} associated with the eigenvalue c. If the algebraic multiplicity of the considered eigenvalue c is equal to one, any discontinuity $[\![\partial u_i/\partial x]\!]$ can be represented as

$$\left[\!\!\left[\frac{\partial u_i}{\partial x}\right]\!\!\right] = aR_i, \quad i = 1,\dots,N, \tag{2}$$

where R_i are the components of a right eigenvector of A_{ij} associated with the eigenvalue c, and a is a scalar factor subsequently referred to as the amplitude of the discontinuity.

Let L_i be the components of a left eigenvector of A_{ij} associated with the same eigenvalue c. Introduce the following quantities on the characteristic curve along which the weak discontinuity propagates [11,12]:

$$\alpha_1 = \frac{L_i}{R_k L_k}\left[R_l \frac{\partial A_{ij}}{\partial u_l}\left(\frac{\partial u_j}{\partial x}\right)^+ + R_j \frac{\partial A_{ij}}{\partial u_l}\left(\frac{\partial u_l}{\partial x}\right)^+ - R_j \frac{\partial B_i}{\partial u_j} + \frac{\mathrm{d}R_i}{\mathrm{d}t}\right], \tag{3}$$

$$\alpha_2 = -\frac{L_i R_j R_l}{R_k L_k}\frac{\partial A_{ij}}{\partial u_l}, \tag{4}$$

where $\mathrm{d}R_i/\mathrm{d}t$ stands for the time derivative of R_i along the characteristic. The amplitude of the discontinuity satisfies the equation

$$\frac{\mathrm{d}a}{\mathrm{d}t} + \alpha_1 a + \alpha_2 a^2 = 0. \tag{5}$$

Note that the right eigenvectors in [12] are assumed to be normalized: $R_i R_i = 1$. This condition does not change Eqs. (3), (4) for α_1, α_2 and is not imposed here. Moreover, the normalization is only possible if all components R_i have the same physical dimension or if they are made nondimensional.

Equation (5) implies that a, α_1, α_2 are functions of time. Alternatively, they can be viewed as functions of the spatial variable x. Replacing the temporal derivative along the characteristic with the spatial one, $\mathrm{d}(\,)/\mathrm{d}t = c\,\mathrm{d}(\,)/\mathrm{d}x$, Eq. (5) can be written in terms of the variable x:

$$c\frac{\mathrm{d}a}{\mathrm{d}x} + \alpha_1 a + \alpha_2 a^2 = 0. \tag{6}$$

If the discontinuity front propagates into a region where the functions u_i are known, the coefficients α_1, α_2 and c in (6) become known functions of x. Equation (6) with known coefficients is the Bernoulli equation which can be solved for $a(x)$. The solution is

$$a(x) = \left(\frac{1}{a_0} + \int_{x_0}^{x} \frac{\alpha_2 \psi}{c}\mathrm{d}\xi\right)^{-1} \psi(x), \tag{7}$$

where

$$\psi(x) = \exp\left(-\int_{x_0}^{x} \frac{\alpha_1}{c}\mathrm{d}\eta\right), \tag{8}$$

and a_0 is the initial amplitude at $x = x_0$.

It is seen from (7) that, if α_2 is not identically zero, (6) may possess solutions which become infinite at a finite x. The critical distance x_c is found from the equation

$$\frac{1}{a_0} + \int_{x_0}^{x_0+x_c} \frac{\alpha_2 \psi}{c}\mathrm{d}\xi = 0. \tag{9}$$

The condition that α_2 must be nonzero for the critical distance to be finite means that some coefficients A_{ij} of system (1) must be functions of u_i, see (4), and, hence, the system must be nonlinear. A solution x_c to (9) is physically relevant if its sign coincides with the sign of c.

3 Constitutive assumptions

We will study the propagation of weak discontinuities in a porous solid saturated with a fluid. The fluid may be a pure liquid (for instance, water) or a liquid with a small amount (few volume percent) of free gas. The total stress is decomposed into the effective stress in the skeleton and an isotropic stress due to the fluid pressure:

$$\boldsymbol{\sigma}_{\text{total}} = \boldsymbol{\sigma} - p\,\mathbf{I}, \tag{10}$$

where $\boldsymbol{\sigma}_{\text{total}}$ and $\boldsymbol{\sigma}$ are, respectively, the total and the effective stress tensors (compressive stresses are negative), p is the fluid pressure (positive for compression), and $\mathbf{I}$ is the unit tensor. The decomposition (10) is justified if the compressibility of the skeleton is much higher than that of the solid phase [13]. This holds, in particular, for soils. According to the effective-stress principle, the constitutive equation for the effective stress tensor in a saturated solid is independent of the pore pressure and is the same as for the dry skeleton.

Let the principal directions of the initial stress tensor coincide with the axes x_1, x_2, x_3 of a rectangular Cartesian coordinate system. The constitutive behaviour of the skeleton is assumed to be such that, if the principal directions of the deformation tensor also coincide with the axes x_1, x_2, x_3, the stress components $\sigma_{12}, \sigma_{13}, \sigma_{23}$ remain zero. Since only such mode of deformation is considered in this paper, it is sufficient to write the constitutive equations as relations between the principal stresses $\sigma_1, \sigma_2, \sigma_3$ and the principal deformations $\varepsilon_1, \varepsilon_2, \varepsilon_3$. The constitutive equations are written in rate form and are taken to be incrementally linear:

$$\dot{\sigma}_1 = \kappa_{11}\dot{\varepsilon}_1 + \kappa_{12}\dot{\varepsilon}_2 + \kappa_{13}\dot{\varepsilon}_3, \tag{11}$$

$$\dot{\sigma}_2 = \kappa_{21}\dot{\varepsilon}_1 + \kappa_{22}\dot{\varepsilon}_2 + \kappa_{23}\dot{\varepsilon}_3, \tag{12}$$

$$\dot{\sigma}_3 = \kappa_{31}\dot{\varepsilon}_1 + \kappa_{32}\dot{\varepsilon}_2 + \kappa_{33}\dot{\varepsilon}_3, \tag{13}$$

where the stiffness coefficients κ_{ij} are functions of the current principal stresses $\sigma_1, \sigma_2, \sigma_3$, and the dot stands for the time derivative.

The permeability of the skeleton is assumed to be low enough to neglect the relative motion between the solid and the fluid phases. The constitutive equation for the pore pressure is then written as

$$\dot{p} = -\frac{K_f}{n}(\dot{\varepsilon}_1 + \dot{\varepsilon}_2 + \dot{\varepsilon}_3), \tag{14}$$

where K_f is the compression modulus of the fluid, and n is the porosity of the skeleton. The modulus K_f may be a function of the fluid pressure p if, for instance, the fluid is not a pure liquid but a liquid with a small amount of free gas.

4 Critical distances for longitudinal waves

As mentioned above, the objective of the present study is to calculate the critical distances for plane, cylindrical and spherical acceleration waves in a solid with pressure-dependent stiffness.

In the plane problem considered in a rectangular Cartesian coordinate system (x_1, x_2, x_3), a longitudinal wave is assumed to propagate along the x_1-axis and to have one nonzero velocity component v_1 and three nonzero stress components $\sigma_{11}, \sigma_{22}, \sigma_{33}$. In a cylindrical coordinate system (r, φ, z), a longitudinal axisymmetric wave has one nonzero velocity component v_r and three nonzero stress components $\sigma_{rr}, \sigma_{\varphi\varphi}, \sigma_{zz}$. Similarly, in a spherical coordinate system (r, φ, θ), a longitudinal spherical wave has one nonzero velocity component v_r and three nonzero stress components $\sigma_{rr}, \sigma_{\varphi\varphi}, \sigma_{\theta\theta}$ with $\sigma_{\varphi\varphi} = \sigma_{\theta\theta}$. The velocity component, the stress components and the pore pressure are functions of the spatial coordinate (x_1 or r) and time.

We write the system of dynamic equations in a form valid simultaneously for all three types of waves by introducing two parameters, m_1 and m_2, which assume certain values for a particular type of waves. In this general system we write v for the velocity component, $\sigma_1, \sigma_2, \sigma_3$ for the stress components, and x for the spatial coordinate. The correspondence between these quantities and the quantities in the particular problems is given in Table 1.

In the absence of mass forces and relative motion between the solid and the fluid constituents, the equation of motion is

$$\frac{\partial v}{\partial t} - \frac{1}{\varrho}\frac{\partial \sigma_1}{\partial x} + \frac{1}{\varrho}\frac{\partial p}{\partial x} - \frac{m_1}{\varrho x}(\sigma_1 - \sigma_2) - \frac{m_2}{\varrho x}(\sigma_1 - \sigma_3) = 0, \tag{15}$$

Table 1 Correspondence between the quantities in system (15)–(19) and in the particular problems

	m_1	m_2	x	v	σ_1	σ_2	σ_3
Plane problem	0	0	x_1	v_1	σ_{11}	σ_{22}	σ_{33}
Cylindrical problem	1	0	r	v_r	σ_{rr}	$\sigma_{\varphi\varphi}$	σ_{zz}
Spherical problem	1	1	r	v_r	σ_{rr}	$\sigma_{\varphi\varphi}$	$\sigma_{\theta\theta}$

where $\varrho = n\varrho_f + (1-n)\varrho_s$ is the mean density of the medium, and ϱ_f, ϱ_s are the densities of the fluid and the solid constituents. In the governing equations in this paper, the convective terms in the material time derivatives are neglected, and the material derivatives are replaced with the partial ones.

Constitutive equations (11)–(13) for the effective stresses and Eq. (14) for the pore pressure are written as

$$\frac{\partial \sigma_1}{\partial t} - \kappa_{11}\frac{\partial v}{\partial x} - m_1\kappa_{12}\frac{v}{x} - m_2\kappa_{13}\frac{v}{x} = 0, \tag{16}$$

$$\frac{\partial \sigma_2}{\partial t} - \kappa_{21}\frac{\partial v}{\partial x} - m_1\kappa_{22}\frac{v}{x} - m_2\kappa_{23}\frac{v}{x} = 0, \tag{17}$$

$$\frac{\partial \sigma_3}{\partial t} - \kappa_{31}\frac{\partial v}{\partial x} - m_1\kappa_{32}\frac{v}{x} - m_2\kappa_{33}\frac{v}{x} = 0, \tag{18}$$

$$\frac{\partial p}{\partial t} + \frac{K_f}{n}\frac{\partial v}{\partial x} + (m_1+m_2)\frac{K_f}{n}\frac{v}{x} = 0, \tag{19}$$

where the stiffness coefficients κ_{ij} are functions of the current principal stresses $\sigma_1, \sigma_2, \sigma_3$, and the compression modulus K_f is a function of the fluid pressure p. Note that, in the case of a spherical wave, in order to ensure the equality $\sigma_{\varphi\varphi} = \sigma_{\theta\theta}$, the coefficients κ_{ij} in (17), (18) as functions of the principal stresses must satisfy the conditions

$$\kappa_{21} = \kappa_{31}, \quad \kappa_{22} + \kappa_{23} = \kappa_{32} + \kappa_{33} \tag{20}$$

whenever $\sigma_2 = \sigma_3$.

System (15)–(19) is of the form (1) with

$$u_1 = v, \quad u_2 = \sigma_1, \quad u_3 = \sigma_2, \quad u_4 = \sigma_3, \quad u_5 = p. \tag{21}$$

The matrix A_{ij} of system (15)–(19) has three zero eigenvalues and two eigenvalues $\pm c$ with

$$c = \sqrt{\frac{1}{\varrho}\left(\kappa_{11} + \frac{K_f}{n}\right)}. \tag{22}$$

The components of the right and the left eigenvectors of the matrix A_{ij} associated with the eigenvalue c are

$$R_2 = -\frac{\kappa_{11}}{c}R_1, \quad R_3 = -\frac{\kappa_{21}}{c}R_1, \quad R_4 = -\frac{\kappa_{31}}{c}R_1, \quad R_5 = \frac{K_f}{nc}R_1, \tag{23}$$

$$L_2 = -\frac{1}{\varrho c}L_1, \quad L_3 = 0, \quad L_4 = 0, \quad L_5 = \frac{1}{\varrho c}L_1, \tag{24}$$

where R_1, L_1 are arbitrary. From (23), (24) it is found that $R_i L_i = 2R_1L_1$.

We will consider the propagation of a weak discontinuity with the positive speed c into a domain where v is zero, $\sigma_1, \sigma_2, \sigma_3, p$ do not depend on x and t, and the density and the porosity are homogeneous. In this case the first two terms on the right-hand side of (3) vanish. Since all quantities ahead of the wave front are homogeneous and, hence, the components of the matrix A_{ij} are constant on the front, we can always take the same right eigenvector and thus have $\mathrm{d}R_i/\mathrm{d}t = 0$ in (3). The only contribution to α_1 is due to the derivatives $\partial B_i/\partial u_j$. Calculating the derivatives (with the density and the porosity treated as constants) and taking into account that $v = 0$ on the front, we obtain

$$\alpha_1(x) = \frac{1}{2\varrho c x}\left[(m_1+m_2)\varrho c^2 + m_1(\kappa_{12}-\kappa_{21}) + m_2(\kappa_{13}-\kappa_{31})\right]. \tag{25}$$

The calculation of α_2 with (4) for system (15)–(19) gives

$$\alpha_2 = \frac{R_1\beta}{2\varrho c^2}, \tag{26}$$

where

$$\beta = \kappa_{11}\frac{\partial \kappa_{11}}{\partial \sigma_1} + \kappa_{21}\frac{\partial \kappa_{11}}{\partial \sigma_2} + \kappa_{31}\frac{\partial \kappa_{11}}{\partial \sigma_3} - \frac{K_f}{n^2}\frac{\mathrm{d}K_f}{\mathrm{d}p}. \tag{27}$$

In order to calculate the critical distance with Eq. (9), it is necessary to specify the initial amplitude of the discontinuity, a_0, at the boundary $x = x_0$ at $t = 0$. We consider a boundary value problem in which the total stress $\sigma_1 - p$ is prescribed at the boundary:

$$\sigma_1(x_0, t) - p(x_0, t) = f(t), \quad t \geq 0, \tag{28}$$

where $f(t)$ is a given function, and $f(0)$ is equal to the initial total stress in the domain $x \geq x_0$.

Let s_0 denote the initial rate of $f(t)$ at $t = 0$:

$$s_0 = \left.\frac{\mathrm{d}f}{\mathrm{d}t}\right|_{t=0}. \tag{29}$$

At the beginning of the propagation, the incipient profile of the wave is linear. The initial gradient of the total stress behind the front produced by the rate s_0 in the immediate vicinity of x_0 is $-s_0\Delta t/\Delta x$, where $\Delta x = c\Delta t$ is the distance travelled by the wave front. This gives

$$\left(\frac{\partial \sigma_1}{\partial x}\right)^- - \left(\frac{\partial p}{\partial x}\right)^- = -\frac{s_0}{c}. \tag{30}$$

On the other hand, the jumps $[\![\partial\sigma_1/\partial x]\!]$, $[\![\partial p/\partial x]\!]$ are proportional to the corresponding components of the right eigenvector of A_{ij}, see (2), that is,

$$\left[\!\!\left[\frac{\partial \sigma_1}{\partial x}\right]\!\!\right] = -\left(\frac{\partial \sigma_1}{\partial x}\right)^- = a_0 R_2, \tag{31}$$

$$\left[\!\!\left[\frac{\partial p}{\partial x}\right]\!\!\right] = -\left(\frac{\partial p}{\partial x}\right)^- = a_0 R_5. \tag{32}$$

Substituting (31), (32) into (30) and using (22), (23), we obtain for the initial amplitude:

$$a_0 = -\frac{s_0}{R_1 \varrho c^2}. \tag{33}$$

With $\alpha_1(x)$ given by (25), introduce a constant

$$\beta_1 = 1 - \frac{\alpha_1 x}{c} = \text{const}. \tag{34}$$

The function $\psi(x)$ defined by (8) then becomes

$$\psi(x) = \exp\left[(\beta_1 - 1)\int_{x_0}^{x} \frac{\mathrm{d}\eta}{\eta}\right] = \left(\frac{x}{x_0}\right)^{\beta_1 - 1}. \tag{35}$$

Equation (9) for the critical distance x_c can now be solved:

$$x_c = \begin{cases} x_0\left(1 + \dfrac{2\varrho^2 c^5 \beta_1}{s_0 x_0 \beta}\right)^{1/\beta_1} - x_0 & \text{if } \beta_1 \neq 0, \\ x_0 \exp\left(\dfrac{2\varrho^2 c^5}{s_0 x_0 \beta}\right) - x_0 & \text{if } \beta_1 = 0. \end{cases} \tag{36}$$

For the plane problem, $m_1 = m_2 = 0$ and, as follows from (25) and (34), $\alpha_1 = 0$, $\beta_1 = 1$. Denoting the critical distance in the plane problem by l_P, we obtain from (36):

$$l_P = \frac{2\varrho^2 c^5}{s_0 \beta}. \tag{37}$$

5 Relations between the critical distances

The existence of plane, cylindrical and spherical waves as specific solutions to the dynamic equations is dictated by the initial state and the constitutive response of the medium at each material point. If the initial state and the constitutive response are such that both plane and cylindrical longitudinal waves can exist in the same body, a simple relation can be established between the critical distances for plane and cylindrical weak discontinuity fronts. Similarly, if both plane and spherical waves can exist, a relation between the corresponding critical distances can be established as well. These relations may be useful in applications as they allow us to estimate immediately the critical distances for cylindrical and spherical fronts once the critical distance for a plane front has been calculated.

In a rectangular Cartesian coordinate system (x_1, x_2, x_3), consider a homogeneous initial state with zero velocity and zero stress components $\sigma_{12}, \sigma_{13}, \sigma_{23}$. Assume the constitutive behaviour of the medium at each point to be the same and such that any deformation with $\varepsilon_{12} = \varepsilon_{13} = \varepsilon_{23} = 0$ does not induce the stress components $\sigma_{12}, \sigma_{13}, \sigma_{23}$. This ensures that plane longitudinal waves can propagate along the x_1-, x_2- or x_3-axis. For deformation with $\varepsilon_{12} = \varepsilon_{13} = \varepsilon_{23} = 0$, the constitutive equations can be written as relations between the principal stresses $\sigma_1, \sigma_2, \sigma_3$ and the principal deformations $\varepsilon_1, \varepsilon_2, \varepsilon_3$ in form (11)–(13).

Introduce a cylindrical coordinate system (r, φ, z) in which the z-axis coincides with the x_3-axis of the Cartesian system and suppose that cylindrical wave fronts can propagate in the same medium. Then, as follows from the static equilibrium condition, the initial stress state must be such that $\sigma_1 = \sigma_2$. Similarly, spherical waves require the initial state to be hydrostatic: $\sigma_1 = \sigma_2 = \sigma_3$. Besides the initial stress state, the existence of cylindrical or spherical waves imposes certain restrictions on the coefficients κ_{ij} of constitutive equations (11)–(13). These restrictions allow us to find the required relations between the critical distances for the three types of waves.

Consider first cylindrical waves in comparison with plane waves propagating along the x_1- or x_2-axis. If the x_1-axis is taken as an r-axis in the cylindrical problem, the evolution of the circumferential stress component for a cylindrical wave is described by constitutive equation (12). Since the velocity is zero on the discontinuity front, the rate of the circumferential stress on the front is $\kappa_{21}\, (\partial v_r/\partial r)^-$. If we trace the same cylindrical wave along the x_2-axis, the evolution of the circumferential stress will be governed by Eq. (11). The rate of this stress on the front will be $\kappa_{12}\, (\partial v_r/\partial r)^-$. Hence, κ_{12} must be equal to κ_{21} on the front. Equations (25) and (34) then give $\beta_1 = 1/2$ for cylindrical waves.

To avoid misunderstanding, it should be emphasized that the existence of cylindrical waves alone does not necessarily mean that $\beta_1 = 1/2$. If the medium has an axisymmetric cylindrical structure which does not admit plane-wave solutions, β_1 may be other than 1/2.

Let l_P and l_C denote, respectively, the critical distances for a plane and a cylindrical fronts with the same initial and boundary conditions. Substituting $\beta_1 = 1/2$ into (36) and using (37), we obtain:

$$l_C = l_P \left(1 + \frac{l_P}{4r_0}\right), \tag{38}$$

where r_0 is the radius at which the boundary condition is prescribed in the cylindrical problem.

A relation between plane and spherical waves can be established in a similar way. Introduce a spherical coordinate system with the same origin as in the Cartesian system. If the x_1-axis is taken as an r-axis in the spherical problem, the evolution of the circumferential stress in the spherical problem will be described by Eqs. (12) and (13). For the rate of this stress on the front these equations give, respectively, $\kappa_{21}\, (\partial v_r/\partial r)^-$ and $\kappa_{31}\, (\partial v_r/\partial r)^-$. If we trace the same spherical wave along the x_2-axis, the rate of the circumferential stress determined by Eqs. (11), (13) will be $\kappa_{12}\, (\partial v_r/\partial r)^-$ and $\kappa_{32}\, (\partial v_r/\partial r)^-$. Finally, considering the x_3-axis and applying Eqs. (11), (12), we obtain $\kappa_{13}\, (\partial v_r/\partial r)^-$ and $\kappa_{23}\, (\partial v_r/\partial r)^-$ for the rate of the circumferential stress. Hence, all six coefficients κ_{ij}, $i \neq j$, must be equal on the front. Equations (25) and (34) then give $\beta_1 = 0$ for spherical waves. Note that, similar to cylindrical waves, the existence of spherical waves alone does not necessarily mean that $\beta_1 = 0$. This equality holds if both plane and spherical waves exist in the same medium.

Let l_P and l_S denote, respectively, the critical distances for a plane and a spherical fronts with the same initial and boundary conditions. Equations (36), (37) with $\beta_1 = 0$ give

$$l_S = r_0 \left[\exp\left(\frac{l_P}{r_0}\right) - 1\right], \tag{39}$$

where r_0 is the radius at which the boundary condition is prescribed in the spherical problem.

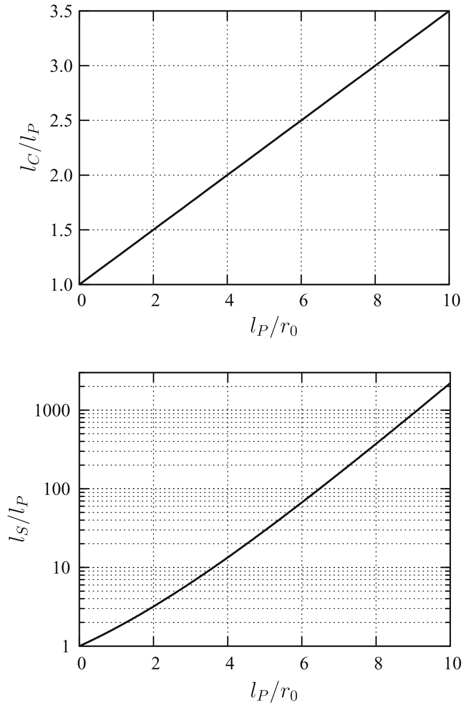

Fig. 1 Critical distances for cylindrical and spherical fronts, l_C and l_S, in comparison with the critical distance for a plane front, l_P, calculated with (38) and (39)

Formulae (38) and (39) allow us to compare the critical distances for the cylindrical and the spherical fronts with that for the plane front depending on the initial radius r_0. In applications, r_0 may represent the radius of a cavity in which the dynamic loading (e.g. caused by an explosion) is generated. Using (38) and (39), it is reasonable to present the ratios l_C/l_P and l_S/l_P as functions of l_P/r_0. These functions are shown in Fig. 1. The distances l_C and l_S are always greater than l_P. As one would expect, if l_P is much smaller than r_0, then both l_C and l_S are close to l_P. It is notable that the growth of l_S/l_P with increasing ratio l_P/r_0 is much faster than that of l_C/l_P.

Below we will calculate the critical distances for particular cases of the pressure dependence of the stiffness typical of granular solids, with emphasis placed on the influence of a small amount of free gas in the pore fluid. Before proceeding to the calculation of the critical distances, we address ourselves to the question of the compressibility of a liquid with a small amount of gas.

6 Compression modulus of the fluid phase

The consideration presented above involves the compression modulus of the pore fluid, K_f. We assume that the pore fluid is water which may contain a small amount of free gas. If the skeleton is fully saturated with water, the compression modulus of the fluid is equal to the modulus of pure water. However, the presence of even less than one volume percent of free gas drastically reduces the compression modulus of the fluid as compared with pure water and, moreover, makes this modulus strongly pressure dependent.

Let K_w, K_g and K_f be the compression moduli of pure water, the free gas and the mixture, respectively. Neglecting the surface tension between the liquid and the gaseous phases and taking the pressure in the liquid phase to be equal to the pressure in the gas, we have, according to the definition of the compression moduli,

$$K_f = -V \frac{\mathrm{d}p}{\mathrm{d}V}, \quad K_g = -V_g \frac{\mathrm{d}p}{\mathrm{d}V_g}, \quad K_w = -V_w \frac{\mathrm{d}p}{\mathrm{d}V_w}, \tag{40}$$

where V_w, V_g, V are the volumes of the water, the gas and the total volume of the fluid. Substituting

$$V = V_w + V_g, \quad \mathrm{d}V = \mathrm{d}V_w + \mathrm{d}V_g \tag{41}$$

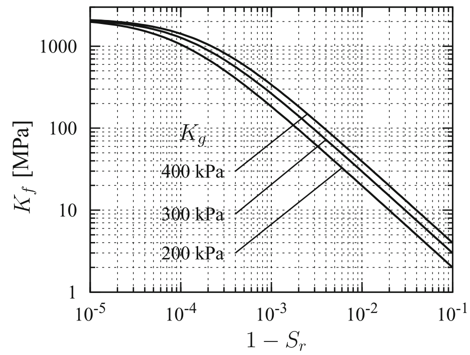

Fig. 2 Compression modulus of the fluid as a function of the gas content

in the first relation in (40), we obtain

$$K_f = \left(V_w + V_g\right)\left(\frac{V_w}{K_w} + \frac{V_g}{K_g}\right)^{-1} = \left(\frac{S_r}{K_w} + \frac{1 - S_r}{K_g}\right)^{-1}, \tag{42}$$

where $S_r = V_w/(V_w + V_g)$ is the degree of saturation.

For an ideal gas, $p_g V_g^{\gamma} = $ conts, where p_g is the absolute pressure of the gas (including the atmospheric pressure), $\gamma = 1$ for isothermal processes, and $\gamma = 1.4$ for adiabatic processes for air. This gives

$$K_g = \gamma p_g. \tag{43}$$

Figure 2 shows the compression modulus of the fluid calculated with (42) as a function of the gas content near full saturation for various values of K_g with $K_w = 2.2$ GPa. For the shown range of K_g, the presence, for instance, of 0.5 volume percent of free gas reduces the compression modulus of the fluid by a factor of 30–55.

The calculation of the critical distance requires, besides K_f, the knowledge of $\mathrm{d}K_f/\mathrm{d}p$, see (27). The quantities V_w, V_g and K_g in (42) are functions of p. Differentiating (42) with respect to p and using (40), (43), we obtain after simple computations

$$\frac{\mathrm{d}K_f}{\mathrm{d}p} = \frac{K_f^2(1 - S_r)\left[S_r(K_w - K_g)^2 + \gamma K_w^2\right]}{K_w^2 K_g^2} \approx \frac{K_f^2(1 - S_r)(S_r + \gamma)}{K_g^2}, \tag{44}$$

where the last approximate expression is justified if $K_g \ll K_w$.

7 Weak discontinuities in a granular medium

In this Section we calculate critical distances for weak discontinuities in a saturated granular medium assuming particular constitutive behaviour of the skeleton and the fluid. The dependence of the stiffness of the skeleton on the effective stress is taken in a form typical of granular skeletons. The fluid is assumed to consist of water with a small amount of free gas. As shown in the previous Section, the compressibility of such a fluid is strongly pressure dependent and differs substantially from the compressibility of pure water. We consider three cases: a granular suspension with zero effective stress, a dry granular skeleton and a saturated granular skeleton. The calculations are performed only for plane fronts. The critical distances for cylindrical or spherical fronts can be obtained from relations (38), (39) or Fig. 1.

Consider first a granular suspension in which a solid skeleton as such is absent and the effective stresses are zero. This may be, for example, the case of a fully liquefied loose saturated soil. With the stiffness coefficients κ_{ij} being identically equal to zero, Eq. (37) for the critical distance reduces to

$$l_P = -\frac{2K_f^{3/2}}{s_0\sqrt{\varrho n}}\left(\frac{\mathrm{d}K_f}{\mathrm{d}p}\right)^{-1}. \tag{45}$$

Formulae (37), (45) show that the critical distance is inversely proportional to the rate of boundary loading s_0. The rates of loading caused, for instance, by an earthquake or an explosion may differ by many

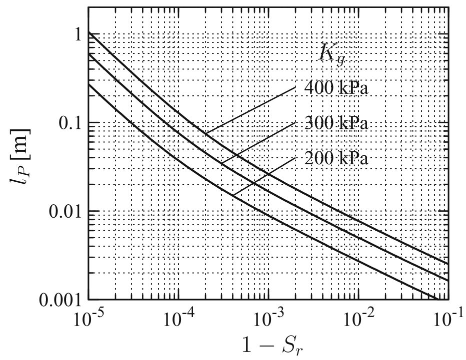

Fig. 3 Critical distance in a granular suspension as a function of the gas content calculated with (45) for the rate of boundary loading $s_0 = -10^4$ MPa/s

Table 2 Parameters used in the numerical calculations

c_{s0} (m/s)	σ_0 (kPa)	ν	m	γ	K_w (GPa)	n	ϱ_s (kg/m^3)	ϱ_f (kg/m^3)
400	−200	0.3	0.5	1.4	2.2	0.38	2650	1000

orders of magnitude, and the same holds for the corresponding critical distances. We present numerical results for $s_0 = -10^4$ MPa/s relevant to blast loading.

The critical distance calculated with (45) using (42), (44) is shown in Fig. 3. The values of ϱ_s, ϱ_f, n and γ used in the calculations are given in Table 2. As the gas content tends to zero, the compressibility of the fluid tends to the pressure-independent compressibility of pure water, the constitutive behaviour of the mixture becomes linear, and the critical distance tends to infinity, as follows from (45) if $\mathrm{d}K_f/\mathrm{d}p \to 0$. The prescribed negative value of s_0 means an increase in the absolute value of stress and therefore corresponds to a compression front. A positive value of s_0 would give a negative critical distance as a formal solution to (9), which would be physically irrelevant as formulae (37), (45) are derived for $c > 0$. This is in accordance with the fact that decompression fronts do not turn into shock fronts.

Consider now a dry granular skeleton. To estimate the critical distances, assume that the initial stress state is hydrostatic, the constitutive behaviour of the skeleton in the vicinity of the initial state is isotropic, and the stiffness moduli depend on the mean effective pressure. The stiffness coefficients $\kappa_{11}, \kappa_{21}, \kappa_{31}$, involved in the plane problem can then be represented in terms of the Lamé constants λ and μ as $\kappa_{11} = \lambda + 2\mu, \kappa_{21} = \kappa_{31} = \lambda$. For granular solids such as sand or soil, the stiffness moduli as functions of the confining pressure obey a power law [14–16]. Based on this fact, we write

$$\lambda(\sigma) = \lambda_0 \left(\frac{\sigma}{\sigma_0}\right)^m, \quad \mu(\sigma) = \mu_0 \left(\frac{\sigma}{\sigma_0}\right)^m, \tag{46}$$

where $\sigma = (\sigma_1 + \sigma_2 + \sigma_3)/3$ is the mean effective stress, $\sigma_1, \sigma_2, \sigma_3$ are the principal stresses, λ_0, μ_0 are reference values of λ, μ at $\sigma = \sigma_0$, and m is an exponent lying typically in the range of 0.5–0.6.

Differentiating λ and μ with respect to $\sigma_1, \sigma_2, \sigma_3$ and substituting the derivatives into (27), we can write β as

$$\beta = \frac{m(1-n)^2 \varrho_s^2 c_s^4 (1+\nu)}{3\,\sigma(1-\nu)}, \tag{47}$$

where ν is the Poisson ratio and

$$c_s = \sqrt{\frac{\lambda + 2\mu}{(1-n)\varrho_s}} \tag{48}$$

is the wave speed in the dry skeleton. With the use of (46), c_s can be written in the convenient form

$$c_s(\sigma) = c_{s0} \left(\frac{\sigma}{\sigma_0}\right)^{m/2}, \tag{49}$$

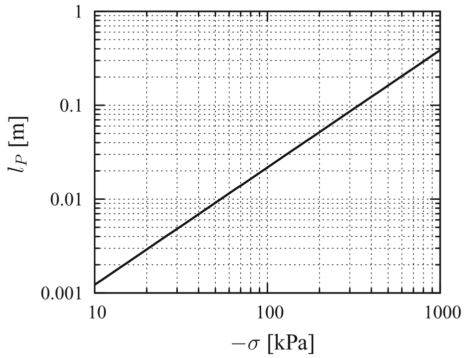

Fig. 4 Critical distance in a dry granular body as a function of the confining pressure for $s_0 = -10^4$ MPa/s

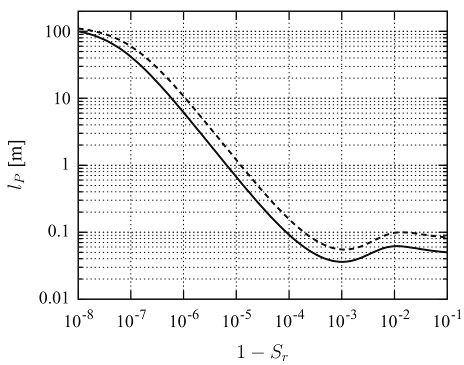

Fig. 5 Critical distance in a saturated granular body as a function of the gas content for $s_0 = -10^4$ MPa/s. *Solid line* $K_g = 300$ kPa, $\sigma = -200$ kPa; *dashed line* $K_g = 400$ kPa, $\sigma = -300$ kPa

where c_{s0} is the value of c_s at $\sigma = \sigma_0$. Thus, for a dry granular medium described by (46), the critical distance determined by (37) is

$$l_P = \frac{6\, c_s \sigma (1-\nu)}{s_0 m (1+\nu)}. \tag{50}$$

Equation (50) alone or in combination with (49) enables us to estimate the critical distance if the speed c_s at a certain stress σ is known or assumed. Although the Poisson ratio ν for granular solids is an indeterminate quantity which depends on many factors, its influence on the critical distance is insignificant: the variation of ν, for instance, between 0.1 and 0.4 changes the ratio $(1-\nu)/(1+\nu)$ in (50) at most by a factor of 2. The critical distance calculated with (50) for $s_0 = -10^4$ MPa/s is shown in Fig. 4 for the constitutive parameters of the skeleton given in Table 2.

If a granular skeleton is saturated with a fluid and the parameters of the constitutive behaviour of the skeleton in Eq. (46) are fixed, the critical distance depends on the effective confining stress σ, the pore pressure (which determines K_g) and the degree of saturation. Figure 5 shows the critical distance in a saturated solid for two combinations of K_g and σ with the same constitutive parameters of the skeleton as in Fig. 4.

As a result of the interplay between the properties of the skeleton and the fluid, the critical distances for the wide range of the gas content from 10^{-1} down to 10^{-4} lie in the narrow range of 4–10 cm. This property is favourable for the theoretical prediction of the critical distance as it does not require the exact knowledge of the degree of saturation within these specific limits. At the same time, the limiting value of the critical distance for full saturation is reached only at a gas content of 10^{-8} and turns out to be by three orders of magnitude greater than at a gas content of 10^{-4}. Besides the fact that the gas content in the second range—between 10^{-4} and 10^{-8}—is immeasurably low, such a small amount of gas cannot be homogeneous in a real solid to give a definite value of the critical distance. In relation to real solids, the questions also arise as to whether the presence of such small amounts of free gas in the pore fluid is physically possible and whether Eqs. (42), (44) still hold true for such amounts of gas. The practical implication of the present result is the following: if the solid skeleton obeys the assumed constitutive relation and the gas content is known to be lower than 10^{-4}, the critical distance will lie between 0.1 and 100 m and is otherwise unpredictable.

8 Concluding remarks

The acceleration-wave approach leads to simple relations between the critical distanced for plane, cylindrical and spherical compression fronts propagating in a solid into a quiescent region. Given the critical distance for a plane front, these relations allow us to estimate the critical distances for cylindrical and spherical fronts for the same boundary loading depending on the radius where the loading is applied.

Besides the wave geometry, the critical distance for a given granular medium depends on the rate of the boundary loading and the degree of saturation. Calculations performed for granular soils reveal two ranges of saturation in which the critical distance behaves differently: with a gas content from 10^{-1} down to 10^{-4}, and below 10^{-4}. The critical distance for plane fronts in the first range depends only slightly on the gas content and changes by a factor of two in the whole range. In contrast, the critical distance in the second range depends strongly on the gas content and increases by three orders of magnitude as the gas content changes from 10^{-4} down to full saturation. From the viewpoint of applications to real soils, such dependence means the indeterminacy of the critical distance within a wide range if the gas content is below 10^{-4}.

If the critical distance is less than the characteristic length in the dynamic problem of interest, the numerical solution imposes specific requirements on both the constitutive model and the numerical algorithm. The constitutive model must adequately describe the pressure dependence of the stiffness, while the numerical algorithm must be capable of solving the dynamic problem with strong discontinuities.

Acknowledgments The study has been carried out within the framework of the project AISIS financed by the German Federal Ministry of Education and Research (BMBF).

References

1. Courant, R., Friedrichs, K.O.: Supersonic Flow and Shock Waves. Springer, New York (1976)
2. Osinov, V.A.: On the formation of discontinuities of wave fronts in a saturated granular body. Continuum Mech. Thermodyn. **10**(5), 253–268 (1998)
3. Chen, P.J.: Growth and decay of waves in solids. In: Truesdell, C. (ed.) Encyclopedia of Physics, vol. VIa/3, Mechanics of Solids III, pp. 303–402. Springer, Berlin (1973)
4. Chen, P.J.: Selected Topics in Wave Propagation. Noordhoff, Leyden (1976)
5. McCarthy, M.F.: Singular surfaces and waves. In: Eringen, A.C. (ed.) Continuum Physics, vol. II, pp. 449–521. Academic Press, New York (1975)
6. Courant, R., Hilbert, D.: Methods of Mathematical Physics, vol. II, Partial Differential Equations. Interscience, New York (1965)
7. Whitham, G.B.: Linear and Nonlinear Waves. Wiley, New York (1974)
8. Boillat, G., Ruggeri, T.: On the evolution law of weak discontinuities for hyperbolic quasi-linear systems. Wave Motion **1**(2), 149–152 (1979)
9. Ruggeri, T.: Stability and discontinuity waves for symmetric hyperbolic systems. In: Jeffrey, A. (ed.) Nonlinear Wave Motion, pp. 148–161. Longman Scientific & Technical, London (1989)
10. Donato, A.: Nonlinear waves. In: Ames, W.F., Rogers, C. (eds.) Nonlinear Equations in the Applied Sciences, pp. 149–174. Academic Press, New York (1992)
11. Wilmanski, K.: Thermomechanics of Continua. Springer, Berlin (1998)
12. Wilmanski, K.: Critical time for acoustic waves in weakly nonlinear poroelastic materials. Continuum Mech. Thermodyn. **17**(2), 171–181 (2005)
13. Zienkiewicz, O.C., Chan, A.H.C., Pastor, M., Schrefler, B.A., Shiomi, T.: Computational geomechanics with special reference to earthquake engineering. Wiley, Chichester (1999)
14. Hardin, B.O., Richart, F.E.: Elastic wave velocities in granular soils. J. Soil Mech. Found. Div., ASCE **89**, SM 1, 33–65 (1963)
15. Lambe, T.W., Whitman, R.V.: Soil Mechanics. Wiley, New York (1969)
16. Santamarina, J.C., Klein, K.A., Fam, M.A.: Soils and Waves. Wiley, Chichester (2001)